Our results raise the possibility of a dynamic role for apoptosis in other morphogenic processes. Indeed, an apoptotic force has been proposed as part of the epithelial strand-pull theory in hair follicles (*21*). Although not all apoptotic processes are related to force generation, we anticipate that apoptotic forces may be important for epithelial fusion in processes such as the development of the adult abdomen of *Drosophila* (*22*). Moreover, we cannot rule out the possibility that apoptotic forces contribute to the tissue-sculpting processes that drive processes such as digit individualization and joint formation. An apoptotic force may also play a beneficial role during wound healing (*11*, *23*) as a source of mechanical tension that promotes tissue reconstruction. We propose that evolution efficiently uses all possible sources of forces for morphogenesis, and that apoptosis in the amnioserosa is one such force that is co-opted to help drive dorsal closure.

References and Notes

1. R. Keller, L. A. Davidson, D. R. Shook, *Differentiation* **71**, 171 (2003).
2. D. P. Kiehart, C. G. Galbraith, K. A. Edwards, W. L. Rickoll, R. A. Montague, *J. Cell Biol.* **149**, 471 (2000).
3. A. Jacinto, A. Martinez-Arias, P. Martin, *Nat. Cell Biol.* **3**, E117 (2001).
4. M. S. Hutson *et al*., *Science* **300**, 145 (2003).
5. X. G. Peralta *et al*., *Biophys. J.* **92**, 2583 (2007).
6. X. G. Peralta, Y. Toyama, D. P. Kiehart, G. S. Edwards, *Phys. Biol.* **5**, 015004 (2008).
7. A. Jacinto *et al*., *Curr. Biol.* **10**, 1420 (2000).
8. J. D. Franke, R. A. Montague, D. P. Kiehart, *Curr. Biol.* **15**, 2208 (2005).
9. M. D. Jacobson, M. Weil, M. C. Raff, *Cell* **88**, 347 (1997).
10. B. H. Reed, R. Wilk, F. Schock, H. D. Lipshitz, *Curr. Biol.* **14**, 372 (2004).
11. J. Rosenblatt, M. C. Raff, L. P. Cramer, *Curr. Biol.* **11**, 1847 (2001).
12. J. M. Abrams, K. White, L. I. Fessler, H. Steller, *Development* **117**, 29 (1993).
13. J. T. Blankenship, S. T. Backovic, J. S. P. Sanny, O. Weitz, J. A. Zallen, *Dev. Cell* **11**, 459 (2006).
14. M. Tamada, T. D. Perez, W. J. Nelson, M. P. Sheetz, *J. Cell Biol.* **176**, 27 (2007).
15. A. H. Brand, N. Perrimon, *Development* **118**, 401 (1993).
16. R. J. Clem, M. Fechheimer, L. K. Miller, *Science* **254**, 1388 (1991).
17. L. Hrdlicka *et al*., *Genesis* **34**, 51 (2002).
18. P. Chen, W. Nordstrom, B. Gish, J. M. Abrams, *Genes Dev.* **10**, 1773 (1996).
19. Materials and methods are available as supporting material on *Science* Online.
20. S. M. Frisch, H. Francis, *J. Cell Biol.* **124**, 619 (1994).
21. K. Stenn, S. Parimoo, S. Prouty, C. Chuong, in *Molecular Basis of Epithelial Appendage Morphogenesis*, C.-M. Chuong, Ed. (Landes Bioscience, Austin, TX, 1998), pp. 111–130.
22. N. Ninov, D. A. Chiarelli, E. Martin-Blanco, *Development* **134**, 367 (2007).
23. D. G. Greenhalgh, *Int. J. Biochem. Cell Biol.* **30**, 1019 (1998).

24. We thank S. Venakides, U. S. Tulu, and A. Rodiriguez-Diaz for useful discussions and A. Boury and R. Montangue for fly husbandry. This research was supported by NIH grant GM33830.

Supporting Online Material

www.sciencemag.org/cgi/content/full/321/5896/1683/DC1
Materials and Methods
SOM Text
Figs. S1 to S4
Tables S1 and S2
Movies S1 to S6
References

27 February 2008; accepted 30 July 2008
10.1126/science.1157052

Clusters of Hyperactive Neurons Near Amyloid Plaques in a Mouse Model of Alzheimer's Disease

Marc Aurel Busche,[1,4] Gerhard Eichhoff,[1,4] Helmuth Adelsberger,[1,4] Dorothee Abramowski,[2] Karl-Heinz Wiederhold,[2] Christian Haass,[3,4] Matthias Staufenbiel,[2] Arthur Konnerth,[1,4]* Olga Garaschuk[1,4]†

The neurodegeneration observed in Alzheimer's disease has been associated with synaptic dismantling and progressive decrease in neuronal activity. We tested this hypothesis in vivo by using two-photon Ca^{2+} imaging in a mouse model of Alzheimer's disease. Although a decrease in neuronal activity was seen in 29% of layer 2/3 cortical neurons, 21% of neurons displayed an unexpected increase in the frequency of spontaneous Ca^{2+} transients. These "hyperactive" neurons were found exclusively near the plaques of amyloid β–depositing mice. The hyperactivity appeared to be due to a relative decrease in synaptic inhibition. Thus, we suggest that a redistribution of synaptic drive between silent and hyperactive neurons, rather than an overall decrease in synaptic activity, provides a mechanism for the disturbed cortical function in Alzheimer's disease.

A progressive decrease in neuronal activity is an established feature of Alzheimer's disease (AD) (*1*, *2*). Even early stages of AD are associated with a decrease in the density of cortical synapses (*3*, *4*) and dendritic spines (*5*). Furthermore, results obtained in various animal models of the disease show amyloid β (Aβ)–mediated inhibition of synaptic currents (*6*–*8*), disruption of synaptic plasticity (*9*, *10*), as well as endocytosis of glutamate receptors (*8*, *11*–*15*). These findings are summarized in the synaptic failure hypothesis suggesting that "AD represents, at least initially, an attack on synapses" (*4*). To test this hypothesis under in vivo conditions, we explored activity of individual cortical neurons in a mouse model of AD. We used double-transgenic APP23xPS45 mice (fig. S1), which overexpress both β-amyloid precursor protein (APP_{Swe}) and mutant presenilin 1 [$Gly^{384}\rightarrow Ala^{384}$ mutation (G384A)] under the control of Thy-1 promoter (*16*). For the simultaneous in vivo visualization of amyloid plaques and cortical neurons (Fig. 1A), we used the multicell bolus loading technique (*17*). We sequentially injected the Ca^{2+} indicator dye Oregon Green 488 BAPTA-1 AM (OGB-1) and the fluorescent marker thioflavin S, known to label fibrillar amyloid deposits (*18*–*21*).

For the assessment of neural network function in APP23xPS45 mice, we analyzed the spontaneous ongoing cortical activity, which is known to be an important determinant of information processing in the brain (*22*–*26*). We simultaneously monitored spontaneously occurring somatic Ca^{2+} transients in many individual cells (Fig. 1, A and B). Such Ca^{2+} transients directly reflect firing of action potentials in neurons (*27*, *28*). In wild-type (WT, 6- to 10-month-old) mice, the pattern of ongoing activity was remarkably stable from cell to cell (Fig. 1, B and C) with a low mean frequency of Ca^{2+} transients (1.41 ± 0.04 transients/min, n = 564 cells). In APP23xPS45 mice of the same age, the pattern of activity was distinctly different from that in the WT control mice (Fig. 1, B to D). In the mutant mice, only 50% of the neurons were active in the normal frequency range, whereas the remaining neurons were at roughly equal proportions, either silent (showing no Ca^{2+} transients over 6-min-long recording periods) or hyperactive [showing transients at much higher frequencies (fig. S2)]. We observed a 16-fold increase in the fraction of hyperactive neurons and a threefold increase in the fraction of silent neurons. We detected no major differences in amplitude (37 ± 4% $\Delta F/F$, where F is fluorescence, and n = 564 cells in WT versus 39 ± 4% and n = 564 in APP23xPS45) or decay time constant (0.96 ± 0.02 s in WT versus 0.83 ± 0.01 s in APP23xPS45) of intracellular Ca^{2+} transients in WT and mutant mice.

[1]Institut für Neurowissenschaften, Technische Universität München (TUM), 80802 München, Germany. [2]Novartis Institutes for Biomedical Research, 4002 Basel, Switzerland. [3]Adolf-Butenandt-Institute, Department of Biochemistry, Laboratory for Neurodegenerative Disease Research, Ludwig-Maximilians-Universität, 80336 München, Germany. [4]Center for Integrated Protein Science, 81377 München, Germany.

*To whom correspondence should be addressed. E-mail: arthur.konnerth@lrz.tum.de

†Present address: Institute of Physiology II, Wilhelmstraße 27, 72074 Tübingen, Germany.

Next, we mapped the distribution of the three types of neurons in relation to the three-dimensionally nearest amyloid plaque (*16*). Hyperactive neurons were found only in close proximity (<60 μm) to the plaque border, whereas silent cells and cells with regular frequencies of Ca^{2+} transients were distributed throughout the cortex (Fig. 2, A and B). At increasing distances from the plaques, the proportion of silent cells gradually increased (Fig. 2C). To address the question of whether changes in neuronal activity pattern occur also in the absence of amyloid plaques, we studied predepositing APP23xPS45 mice (1.5 to 2 months of age; fig. S1, D to F). At this age the cortical activity was normal, without any difference in the amplitude, the kinetics, or the frequency of spontaneous Ca^{2+} transients (fig. S3). Furthermore, the behavioral performance was inconspicuous: At 2 months of age, APP23xPS45 mice performed normally when tested in the discriminatory water maze task [spatial memory test (*29*)] and in the Y maze [working memory test (*30*); fig. S4]. In contrast, 6- to 8-month-old Aβ-depositing mice showed a significantly reduced performance in both memory tests. In the water maze test, APP23xPS45 mice not only made fewer correct choices but also needed a significantly longer time for making a decision (fig. S4, A and B).

What are the mechanisms underlying neuronal hyperactivity in APP23xPS45 mice? The increased frequency of Ca^{2+} transients may be caused by spontaneous Ca^{2+} release from overfilled intracellular Ca^{2+} stores because the G384A mutation was shown to abolish the presenilin-mediated Ca^{2+} leak from intracellular Ca^{2+} stores (*31*). This Ca^{2+} leak is important to maintain the physiological filling state of the stores (*32*). However, we found that in 4/4 mutant mice the sodium channel blocker tetrodotoxin (TTX) completely and reversibly blocked all Ca^{2+} transients of hyperactive neurons, indicating that they were exclusively generated by action potential firing. This posed the next question of whether in hyperactive neurons there is an increased neuronal excitability leading to strong intrinsic firing or whether the Ca^{2+} transients are driven by synaptic activity. This question was answered by the observation that the Ca^{2+} transients of hyperactive neurons were completely abolished by the application of the ionotropic glutamate receptor blockers 6-cyano-7-nitroquinoxaline-2,3-dione (CNQX) and D,L-2-amino-5-phosphonovaleric acid (APV) (n = 7 cells in five mice) (Fig. 3A). The synaptic origin of the Ca^{2+} transients in hyperactive neurons was further supported by the finding that, in a given peri-plaque region, all neuronal Ca^{2+} transients were strictly correlated with the respective neuropil signals, known to reflect primarily the activity of presynaptic fibers (*27*) (Fig. 3, B and C; n = 6 experiments). The activity of hyperactive neurons surrounding a given plaque was correlated (Fig. 3, B and D). Importantly, the spontaneous as well as glutamate-induced Ca^{2+} transients detected in hyperactive neurons were very similar to those recorded in the "normal" neurons (figs. S5 and S6), indicating the absence of any major increase in intrinsic excitability in hyperactive neurons. Thus, a possible explanation for the neuronal hyperactivity may be an impairment of synaptic inhibition. In order

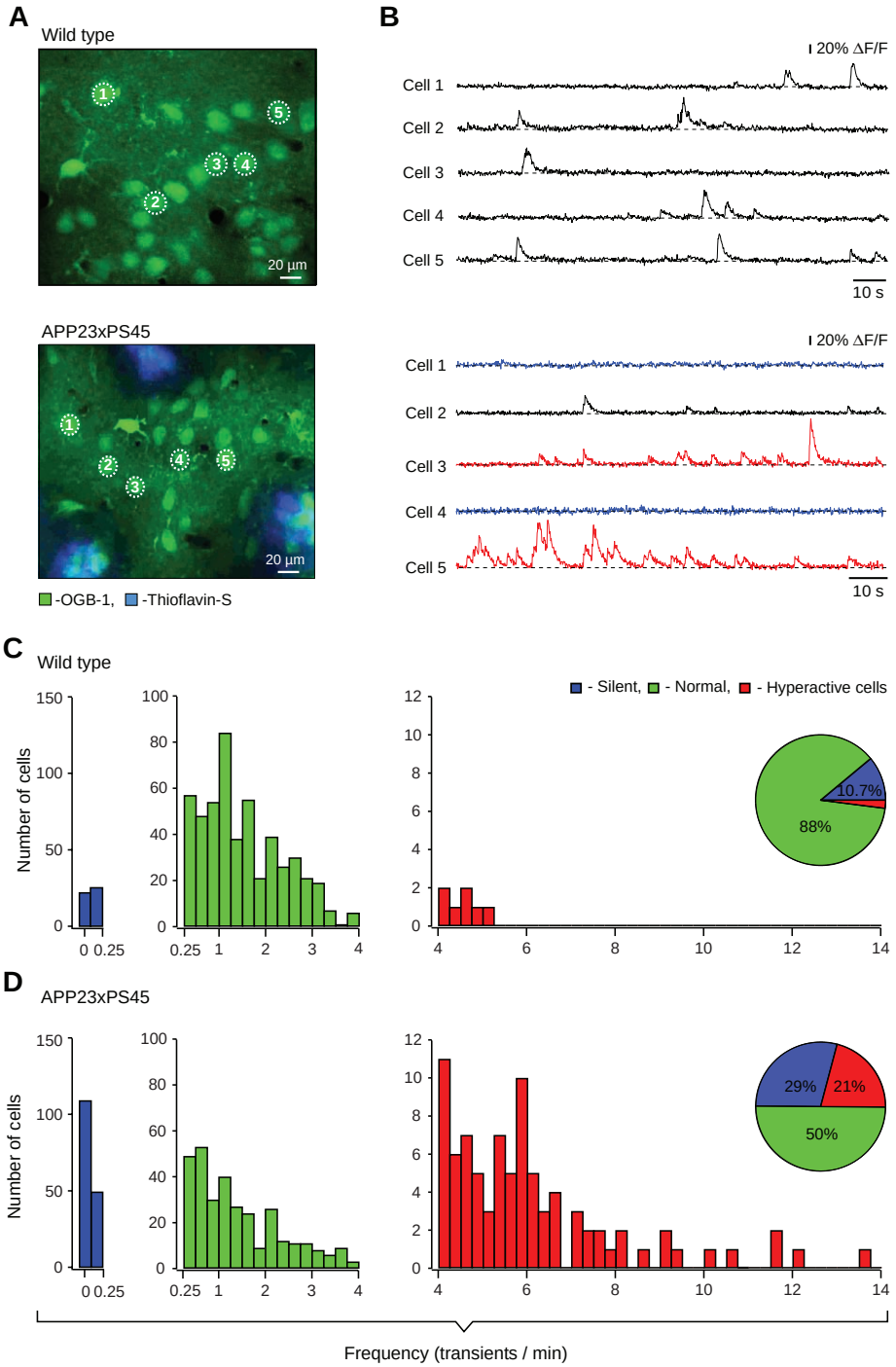

Fig. 1. Altered activity of layer 2/3 neurons in APP23xPS45 mice. (**A** and **B**) Spontaneous Ca^{2+} transients (B) recorded in vivo in the corresponding neurons of the frontal cortex shown in (A) in a WT (top) and a APP23xPS45 (bottom) mouse. Traces in (B) bottom are color-coded to mark neurons that were either inactive during the recording period (blue) or showed an increased frequency of Ca^{2+} transients (red). (**C** and **D**) Histograms showing the frequency distribution of Ca^{2+} transients in WT and APP23xPS45 mice (in both cases n = 564 cells). There is a substantial increase in the amount of silent and hyperactive neurons in APP23xPS45 mice. (Insets) Pie charts showing the relative proportion of silent, normal, and hyperactive neurons in WT (n = 10) and APP23xPS45 (n = 20) mice.

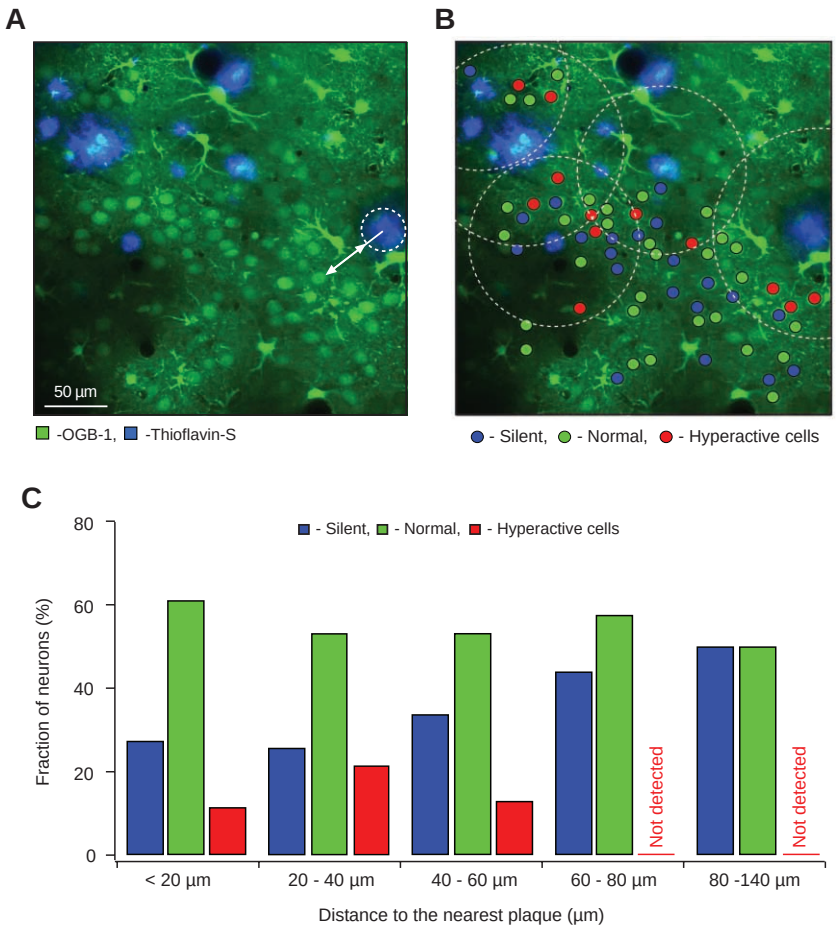

Fig. 2. Spatial distribution of silent and hyperactive neurons in APP23xPS45 mice. (**A**) Maximal projection image (100- to 130-μm depth) of layer 2/3 in the frontal cortex of an APP23xPS45 mouse. To measure the distance from the plaque to the recorded cell, we fitted the plaque with a circle and measured the distance (arrow) between the plaque border and the middle of the cell. The cortical area located above and below the imaged plane (55- to 175-μm depth) was also scanned to assure that plaques shown were nearest to the recorded neurons. (**B**) Activity map of this region with neurons color-coded according to the frequency of their Ca^{2+} transients. The broken line circles are centered at the respective plaques and delineate the area located less than 60 μm from the plaque border. (**C**) Bar graph showing the abundance of silent, normal, and hyperactive neurons at different distances from the border of the nearest plaque (n = 422 cells).

to test whether hyperactive neurons still receive synaptic inhibition, we locally applied diazepam, a benzodiazepine that increases the open probability of γ-aminobutyric acid type A ($GABA_A$) receptor channels. This treatment markedly reduced the activity of hyperactive neurons (from 6.10 ± 0.28 transients/min, n = 13 cells in five mice, to 1.52 ± 0.36 transients/min; Fig. 3, E and F). Application of the $GABA_A$ receptor antagonist gabazine increased the frequency of Ca^{2+} transients in all three types of neurons to the same level of 30 to 40 transients/min (Fig. 3, G and H). However, the relative frequency increase in hyperactive neurons (5.7-fold, n = 9 cells in four mice) was distinctly smaller compared with the frequency increase in normally active cells (16.3-fold, n = 13 cells in four mice). Thus, taken together, our results suggest that an impaired synaptic inhibition, rather than intracellular Ca^{2+} release from store signaling or intrinsic firing, underlies hyperactivity.

What are the mediator(s) of the synaptically driven neuronal hyperactivity? The list of candidate molecules includes (i) soluble Aβ42 oligomers accumulating in the vicinity of amyloid plaques (*33*, *34*) as well as (ii) different proinflammatory mediators released from activated microglia and astrocytes. The latter include cytokines, reactive oxygen species, complement factors, free radicals, and nitric oxide (*35*). These factors most likely cause an anatomical remodeling of both excitatory and inhibitory synaptic inputs that underlies the observed changes in neuronal function. Such a remodeling has been observed in two different mouse models of AD. In APP23 mice, axons of entorhinal (excitatory) neurons showed a hyperinnervation of the thalamic regions surrounding Aβ plaques (*36*), whereas in hAPP mice axonal sprouting of GABAergic interneurons was found in the hippocampal dentate gyrus (*37*).

In conclusion, the study of the in vivo function of individual cortical neurons in a mouse model of AD revealed an increase in neuronal activity in the direct vicinity of Aβ plaques. Not only do hyperactive neurons fire more frequently, they also do this in a correlated manner, thus increasing the risk for seizurelike activity. Indeed, AD patients are known to have an increased incidence of epileptic seizures (*38*, *39*), and spontaneous nonconvulsive seizures have been observed in the cortex and hippocampus of another AD mouse model (*37*). The hyperactive neurons are likely candidates to trigger this pathological activity. Besides, hyperactivity may contribute to the calcium overload recently observed in neurites surrounding Aβ plaques (*40*). Together with the silent neurons, which are distributed throughout the cortex, hyperactive neurons comprise up to 50% of neuronal population, revealing a substantial dysfunction of neuronal network in APP23xPS45 mice. A strict correlation was observed between the formation of amyloid plaques, the appearance of hyperactive neurons, and the impairment of the animal's learning capability. Furthermore, the peri-plaque regions appear to act like distinct functional compartments of the diseased mouse brain. These compartments are not only "reservoirs" of bioactive molecules, attracting and activating microglia as well as causing loss of dendritic spines and axonal dystrophies (*41*), they also modify the functional properties of neurons, making them hyperactive.

References and Notes

1. D. Prvulovic, V. Van de Ven, A. T. Sack, K. Maurer, D. E. Linden, *Psychiatry Res.* **140**, 97 (2005).
2. D. H. Silverman *et al.*, *JAMA* **286**, 2120 (2001).
3. C. A. Davies, D. M. Mann, P. Q. Sumpter, P. O. Yates, *J. Neurol. Sci.* **78**, 151 (1987).
4. D. J. Selkoe, *Science* **298**, 789 (2002).
5. R. D. Terry *et al.*, *Ann. Neurol.* **30**, 572 (1991).
6. A. Y. Hsia *et al.*, *Proc. Natl. Acad. Sci. U.S.A.* **96**, 3228 (1999).
7. E. H. Chang *et al.*, *Proc. Natl. Acad. Sci. U.S.A.* **103**, 3410 (2006).
8. F. Kamenetz *et al.*, *Neuron* **37**, 925 (2003).
9. D. M. Walsh *et al.*, *Nature* **416**, 535 (2002).
10. J. S. Jacobsen *et al.*, *Proc. Natl. Acad. Sci. U.S.A.* **103**, 5161 (2006).
11. H. Hsieh *et al.*, *Neuron* **52**, 831 (2006).

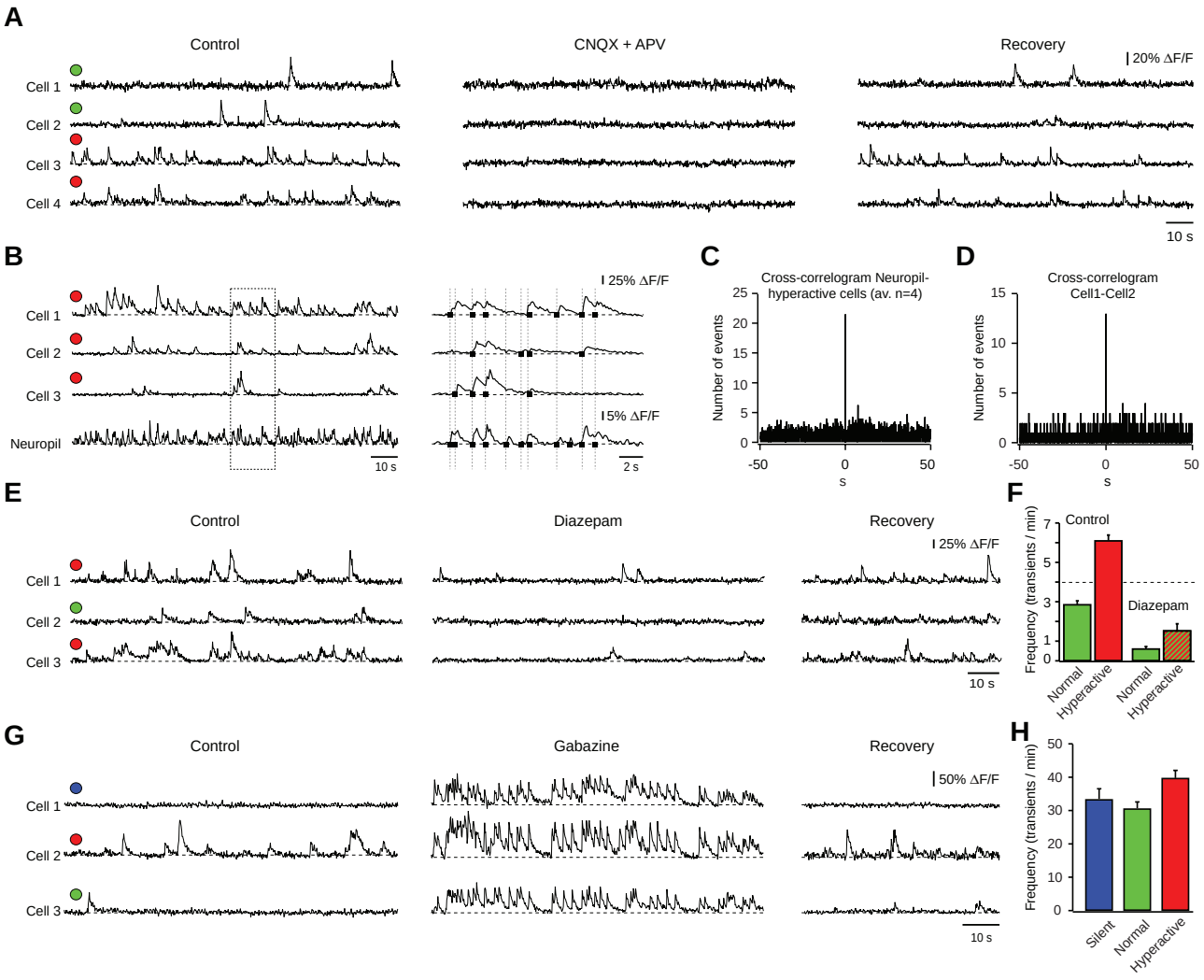

Fig. 3. Synaptic mechanisms of hyperactivity. (**A**) Spontaneous Ca^{2+} transients in layer 2/3 neurons before, during, and after a local iontophoretic application of CNQX and APV. Here and below, the colored circles indicate the type of neuron (blue, silent; green, normal; and red, hyperactive). (**B**) Activity pattern in a region with many hyperactive neurons. Each Ca^{2+} transient in the cell is correlated with a transient in the neuropil. Each black square marks the beginning of a Ca^{2+} transient. (**C** and **D**) Cross-correlograms of digitized traces showing that Ca^{2+} transients in individual hyperactive neurons are correlated with each other and with Ca^{2+} transients in the neuropil. (**E**) Spontaneous Ca^{2+} transients before, during, and after a local pressure application of diazepam. (**F**) Summary graph illustrating the effect of diazepam on the frequency of Ca^{2+} transients (n = 21 normal and 13 hyperactive neurons). (**G**) Spontaneous Ca^{2+} transients before, during, and after a local iontophoretic application of gabazine (60 s, 500 μM in the application pipette). (**H**) Summary graph illustrating the effect of gabazine on the frequency of Ca^{2+} transients (n = 6 silent, 13 normal, and 9 hyperactive neurons). Error bars in each panel represent SEM.

12. S. Oddo *et al.*, *Neuron* **39**, 409 (2003).
13. V. Nimmrich *et al.*, *J. Neurosci.* **28**, 788 (2008).
14. G. M. Shankar *et al.*, *J. Neurosci.* **27**, 2866 (2007).
15. E. M. Snyder *et al.*, *Nat. Neurosci.* **8**, 1051 (2005).
16. Materials and methods are available as supporting material on *Science* Online.
17. C. Stosiek, O. Garaschuk, K. Holthoff, A. Konnerth, *Proc. Natl. Acad. Sci. U.S.A.* **100**, 7319 (2003).
18. R. H. Christie *et al.*, *J. Neurosci.* **21**, 858 (2001).
19. J. Grutzendler, K. Helmin, J. Tsai, W. B. Gan, *Ann. N. Y. Acad. Sci.* **1097**, 30 (2007).
20. O. Garaschuk, R. I. Milos, A. Konnerth, *Nat. Protoc.* **1**, 380 (2006).
21. G. Eichhoff, M. A. Busche, O. Garaschuk, *Eur. J. Nucl. Med. Mol. Imaging* **35**, 599 (2008).
22. A. Arieli, A. Sterkin, A. Grinvald, A. Aertsen, *Science* **273**, 1868 (1996).
23. I. Ferezou, S. Bolea, C. C. Petersen, *Neuron* **50**, 617 (2006).
24. J. Anderson, I. Lampl, I. Reichova, M. Carandini, D. Ferster, *Nat. Neurosci.* **3**, 617 (2000).
25. D. Ji, M. A. Wilson, *Nat. Neurosci.* **10**, 100 (2007).
26. L. Marshall, H. Helgadottir, M. Molle, J. Born, *Nature* **444**, 610 (2006).
27. J. N. Kerr, D. Greenberg, F. Helmchen, *Proc. Natl. Acad. Sci. U.S.A.* **102**, 14063 (2005).
28. T. R. Sato, N. W. Gray, Z. F. Mainen, K. Svoboda, *PLoS Biol.* **5**, e189 (2007).
29. M. Arns, M. Sauvage, T. Steckler, *Behav. Brain Res.* **106**, 151 (1999).
30. O. Wirths, H. Breyhan, S. Schafer, C. Roth, T. A. Bayer, *Neurobiol. Aging* **29**, 891 (2008).
31. O. Nelson *et al.*, *J. Clin. Investig.* **117**, 1230 (2007).
32. H. Tu *et al.*, *Cell* **126**, 981 (2006).
33. R. Kayed *et al.*, *Science* **300**, 486 (2003).
34. C. Haass, D. J. Selkoe, *Nat. Rev. Mol. Cell Biol.* **8**, 101 (2007).
35. M. T. Heneka, M. K. O'Banion, *J. Neuroimmunol.* **184**, 69 (2007).
36. A. L. Phinney *et al.*, *J. Neurosci.* **19**, 8552 (1999).
37. J. J. Palop *et al.*, *Neuron* **55**, 697 (2007).
38. J. C. Amatniek *et al.*, *Epilepsia* **47**, 867 (2006).
39. D. A. Lozsadi, A. J. Larner, *Dement. Geriatr. Cogn. Disord.* **22**, 121 (2006).
40. K. V. Kuchibhotla *et al.*, *Neuron* **59**, 214 (2008).
41. M. Meyer-Luehmann *et al.*, *Nature* **451**, 720 (2008).

42. A.K. is a Carl-von-Linde Fellow of the Institute for Advanced Study of the TUM. We thank L. B. Cohen for comments on the manuscript. Supported by grants from the Deutsche Forschungsgemeinschaft (SFB 596, GA 654/1-1, and HO 2156/2-1) and the Helmholtz Gemeinschaft.

Supporting Online Material

www.sciencemag.org/cgi/content/full/321/5896/1686/DC1
Materials and Methods
Figs. S1 to S6
References

7 July 2008; accepted 19 August 2008
10.1126/science.1162844